Journal of Materials Chemistry B

Accepted Manuscript



This is an *Accepted Manuscript*, which has been through the Royal Society of Chemistry peer review process and has been accepted for publication.

Accepted Manuscripts are published online shortly after acceptance, before technical editing, formatting and proof reading. Using this free service, authors can make their results available to the community, in citable form, before we publish the edited article. We will replace this Accepted Manuscript with the edited and formatted Advance Article as soon as it is available.

You can find more information about *Accepted Manuscripts* in the **Information for Authors**.

Please note that technical editing may introduce minor changes to the text and/or graphics, which may alter content. The journal's standard <u>Terms & Conditions</u> and the <u>Ethical guidelines</u> still apply. In no event shall the Royal Society of Chemistry be held responsible for any errors or omissions in this *Accepted Manuscript* or any consequences arising from the use of any information it contains.



Journal of Materials Chemistry B

RSCPublishing

ARTICLE

Cite this: DOI: 10.1039/x0xx00000x

Received ooth January 2014, Accepted ooth January 2014

DOI: 10.1039/x0xx00000x

www.rsc.org/

Graphene loading water-soluble phthalocyanine for dual-modality photothermal/photodynamic therapy via a one-step method

Bang-Ping Jiang,‡ Lan-Fang Hu,‡ Dong-Jin Wang, Shi-Chen Ji, Xing-Can Shen* and Hong Liang*

In this paper, we present a new and facile one-step method for the fabrication of a water-soluble graphene-phthalocyanine (GR-Pc) hybrid material by simply sonicating GR with a hydrophilic Pc, tetrasulfonic acid tetrasodium salt copper phthalocyanine (TSCuPc). In the resultant hybrid material, TSCuPc is coated on the skeleton of pristine GR via non-covalently π - π interaction, detailedly characterized by UV-vis/Raman spectra, X-ray photoelectron spectroscopy (XPS), *etc.* The obtained GR-Pc hybrid (GR-TSCuPc) is applied for photothermal therapy (PTT) and photodynamic therapy (PDT). In this PTT/PDT system, both GR and TSCuPc operate as multifunctional agents: GR acts as a photosensitizer carrier and PTT agent, while TSCuPc acts as a hydrophilic PDT agent. Furthermore, the results of cell viability show that the phototherapy effect of GR-TSCuPc is observably higher than that of free TSCuPc, indicating that combined noninvasive PTT/PDT exhibits better anti-cancer efficacy *in vitro*. Such results highlight that this work provide a facile method to develop efficacious dual-modality carbon nanoplatform for developing cancer therapeutics.

Introduction

The ever-increasing demand for advances in cancer treatment has triggered enormous research efforts to develop nanoplatforms that integrate several different therapeutic modalities into a single system, which can exceed the individual therapeutic response of each system and may lead to enhanced therapeutic efficiency. 1-4 Among them, combining noninvasive photothermal therapy (PTT) and photodynamic therapy (PDT) in one system has been a research hotspot in the forefront of medical science and materials science due to their unique advantages over conventional therapy methods such as remote controllability, improved selectivity, and low systemic toxicity.⁵⁻⁷ PTT and PDT are two major types of phototherapy methods that are currently used in clinics.^{5,8} PTT is a hyperthermia treatment that can cause cells damage by heating tissue, which is achieved through the conversion of energy absorbed from photons by PTT agent.^{5,8-11} Similar to PTT, PDT is also a form of phototherapy through absorbing photons by photosensitizer (PS), however, rather than generating heat, it results in damage of the targeted tissue that production of reactive oxygen species (ROS) such as singlet oxygen (¹O₂) or free radicals by transferring the photon energy to surrounding oxygen molecules. 7,12-14

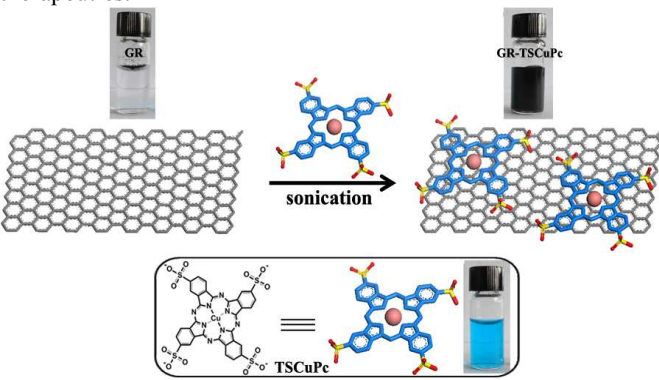
Graphene (GR) are one kind of two-dimensional carbon nanomaterials with sp²-hybridized carbon atoms arranged in a honeycomb pattern that have been intensively explored in recent years for applications in many different fields including nanoelectronics, ¹⁵ nanocomposites, ^{16–18} sensors, ^{19–21} *etc*. Owing

to their high optical absorption in the near infrared region (NIR), a new direction for GR is in the field of nanomedicine, which can act as a photothermal agent and efficiently convert NIR light into heat, thus resulting in hyperthermia to cells and surrounding tissues. 22,23 Up to now, several methods have been developed to construct dual-modality nanoplatforms based on GR to improve water solubility of GR and achieve dualmodality therapy. 11,24-26 Such preparation methods offer an exciting opportunity for combinatorial therapy based on GR. However, the methods are often relatively complex and require multiple steps, including of chemical oxidization of GR, loading hydrophobic PS or drug molecules, and grafting hydrophilic agent are generally needed.^{24–26} Moreover, oxidization of GR may lead to inferior physical and electronic properties due to the damage of GR structures.^{27,28} Therefore, facile methods, especially facile one-step methods that do not need to chemically oxidize GR are expected to achieve dualmodality therapy with excellent solubility while retaining the desirable intrinsic properties of GR.27 Considering that GR possess a high and accessible π -electron surface, it is feasible for GR to non-covalently π – π stack with water-soluble planar aromatic molecules to implement multifunctions. 27,29

Phthalocyanines (Pc), one kind of aromatic macrocycle with two-dimensional and 18 π -electron structure, have been widely investigated as PS for PDT due to a variety of remarkable properties including physical and chemical properties. ^{30,31} However, their applications for PDT in physiological

environments have been limited due to the loss of their ROS generation efficiency, which are mainly resulted from their severe self-aggregation in aqueous environments. 31,32 Therefore, enormous work has been performed to develop alternative strategies to effectively protect them from selfaggregation. 31,33,34 It is found that bonding Pc on the surface of carbon nanomaterials is an efficacious strategy to not only restrict the self-aggregation of Pc but also fabricate the functionalized nanoplatforms.^{27,34} A typical example was presented to address this issue by Tuantranont and co-workers that the π - π bonded water-soluble Pc with GR through electrolytic exfoliation.²⁷ However, to the best of our knowledge, it has not yet been reported that non-oxidizing GR directly functionalized by water-soluble Pc are applied to construct dual-modality nanoplatforms for PTT and PDT via non-covalent π – π stacking, where water-soluble simultaneously acts as hydrophilic agent and PDT agent.

Building from these ideas, we herein present a new and facile one-step method for the preparation of a water-soluble GR-Pc hybrid material by sonication, where a hydrophilic Pc, tetrasulfonic acid tetrasodium salt copper phthalocyanine (TSCuPc), is non-covalently coated on the skeleton of pristine GR via π - π interaction. The resultant GR-TSCuPc hybrid can be further applied as a phototherapy system, where dual-modality therapy combined noninvasive PTT and PDT is expected to be achieved and improve the cancer cell killing efficacy. Therefore, our study may provide a facile method to develop efficacious dual-modality nanoplatform for cancer therapeutics.



Scheme 1. Schematic illustration of the preparation of GR-TSCuPc hybrid: TSCuPc coated on the surface of GR via non-covalent π - π stacking. Photographs show the GR, TSCuPc and GR-TSCuPc dispersed in aqueous solution.

Results and Discussion

Characterization of GR-TSCuPc. The GR-TSCuPc hybrid was fabricated by non-covalently coating TSCuPc on the surface of GR via a facile one-step method, as depicted in Scheme 1. An intuitive comparison between GR, TSCuPc, and GR-TSCuPc is represented in Scheme 1 (photographs). The high solubility of GR into aqueous solution further reveals that the surface of GR is covered by TSCuPc.

We primarily performed the UV-vis spectra of free TSCuPc and GR-TSCuPc in aqueous solution to characterize the optical

properties and identify the chemical structure of the hybrid materials, shown in Fig. 1.³⁵ Free TSCuPc exhibits the typical Q band of phthalocyanine derivatives in the wavelength region between 500 and 750 nm, ^{36,37} which consists of two bands, one with a prominent peak at 629 nm and the other with a satellite shoulder at 663 nm, corresponding to the presence of a dimer and a monomer of TSCuPc, respectively.^{38,39} However, for GR–TSCuPc, the absorption band of the dimer peak largely disappears, whereas the absorption band of the monomer peak broadens and weakens, accompanying a red shift to around 705 nm. The phenomena indicate strong interactions between GR and TSCuPc, which results in reduced aggregation of TSCuPc, similar to previous reports.^{40,41}

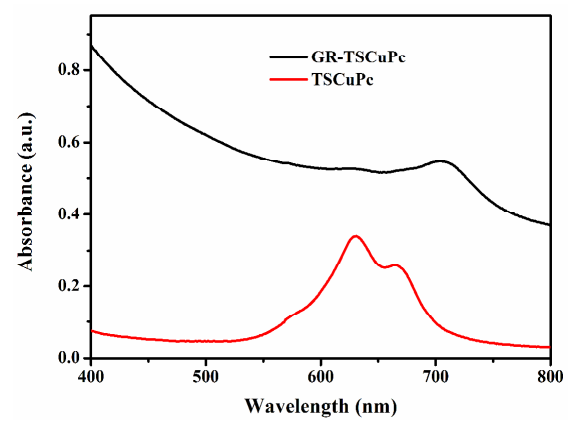


Fig. 1 UV–vis spectra of free TSCuPc and GR–TSCuPc with equivalent TSCuPc concentration of 5 μg mL⁻¹ in aqueous solution.

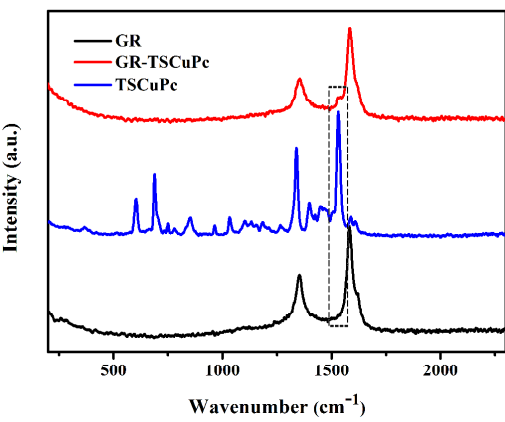
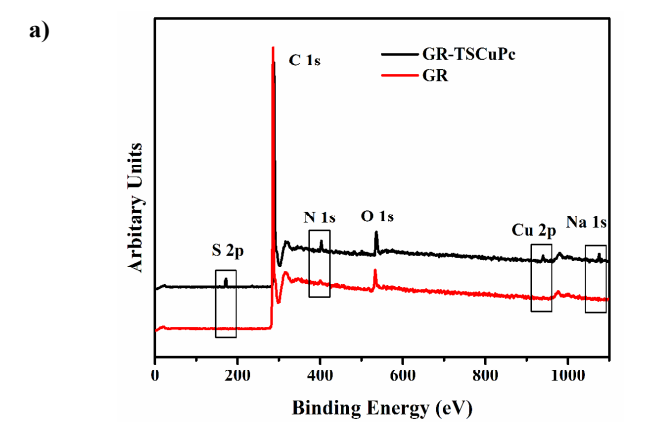


Fig. 2 Raman spectra of GR, free TSCuPc and GR-TSCuPc, $\lambda_{ex} = 514$

The GR–TSCuPc hybrid was detailedly characterized by Raman spectra and X-ray photoelectron spectroscopy (XPS). Fig. 2 shows the Raman spectra of pristine GR, free TSCuPc and GR–TSCuPc. The spectra of both pristine GR and GR–TSCuPc show a D band at 1353 cm⁻¹ and a G band at 1582 cm⁻¹, which are related to surface defects and sp²-hybridized carbon stretching vibrations of GR, respectively.²⁷ The ratio between the intensities of the G and D bands, I_G/I_D , is an index of the defect density in GR.^{42,43} The I_G/I_D ratio of pristine GR is 1.62, whereas it is 1.91 for GR–TSCuPc, which is about 20% higher than that of pristine GR, suggesting a larger average sp² domain size and lower defect density of GR in the hybrid structure.

Moreover, a new weak peak, assigned to pyrrol C=C stretching mode of TSCuPc at 1531 cm⁻¹, can be observable in the Raman spectrum of GR-TSCuPc, due to the peak overlapping between GR and TSCuPc in GR-TSCuPc. These results of Raman spectra further confirmed the successful preparation of GR-TSCuPc hybrid.



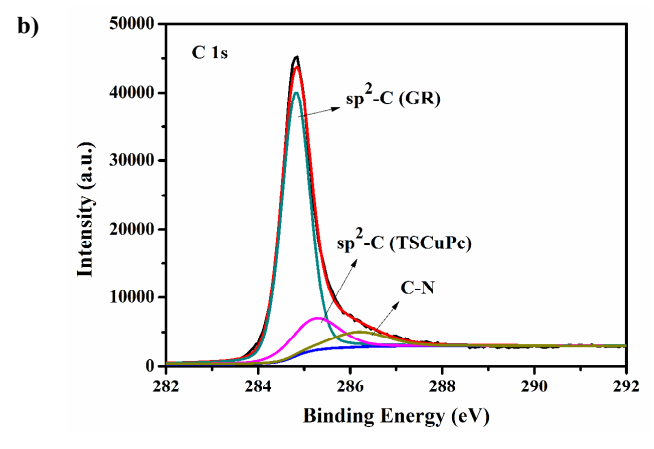
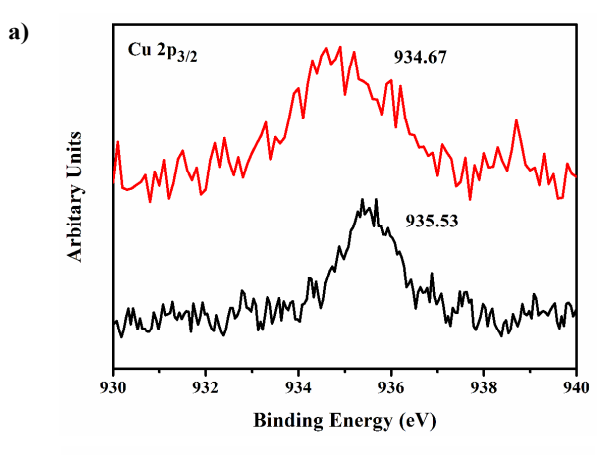


Fig. 3 (a) XPS survey spectra of GR and GR-TSCuPc. (b) High resolution C 1s spectra of GR-TSCuPc.

XPS represents an effective technique for surface analysis, so the experiments of XPS were employed to give evidence of GR–TSCuPc hybrid. Besides the core-level contributed by C 1s and O 1s, the XPS survey spectrum of GR–TSCuPc shows the photoelectrons collected from S 2p, Cu 2p_{3/2}, Na 1s core-levels, which belong to characteristic signals of TSCuPc (Fig. 3a), confirming the presence of TSCuPc at the surface of GR. The C 1s spectrum of GR–TSCuPc can be deconvoluted into three peak components with binding energies at about 284.8, 285.2 and 286.2 eV (Fig. 3b). The peak at 284.8 eV is assigned to sp²-hybridized carbon of GR, which is similar to the pristine GR showing a high energy region at the site. 44 The peaks at 285.2 and 286.2 eV are contributed by sp²-hybridized carbon and C–N of Pc, respectively. 45,46

The binding energy is related to the electron density around the nucleus, in which the lower electronic density is provided with the higher binding energy.³⁷ In the spectrum of the hybrid, the binding energy of the Cu 2p_{3/2} peak is increased by 0.86 eV as compared to that of free TSCuPc (Fig. 4). Such a high

binding energy shift indicates that the electronic density of Pc ring decreased, ascribed to the charge transfers from TSCuPc to GR. This can be also confirmed by the N 1s spectrum, where the binding energy of the N 1s spectrum of GR–TSCuPc, consisting of two peaks (399.0 and 400.1 eV) assigned to two groups of four nitrogen atoms in different chemical environments, 47 suffers pronounced upfield shifts about 0.25 eV compared to that of free TSCuPc. In addition, the S 2p spectrum in the composite is less affected by the decreased charge density on the Pc, and slightly shifted by 0.05 eV toward higher binding energy (Fig. S1), probably owing to the electron-withdrawing property of sufonate groups in TSCuPc. 37,48,49 Overall, the higher energy shifts in Cu 2p and N 1s are consistent with the reported charge transfer phenomena. 36



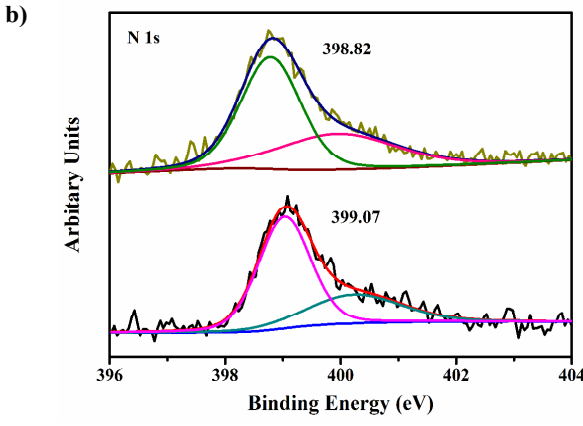


Fig. 4 XPS spectra of Cu $2p_{3/2}$ (a) and N 1s (b) levels in TSCuPc. For each set of core level spectra the upper spectra pertain to TSCuPc only and the lower spectra to GR–TSCuPc.

The amount of TSCuPc in GR-TSCuPc was estimated by thermogravimetric analysis (TGA). As observed in the thermogravimetric curve in Fig. 5, the pristine GR shows no obvious weight-loss step, suggesting that the GR does not decompose. The curve of TSCuPc present three major weight loss steps from 50 to 260 °C, 420 to 540 °C and 580 to 730 °C, which may correspond to the desorption of adsorbed water and the decomposition of TSCuPc, respectively. The thermogram of GR-TSCuPc exhibits some similarities to that of TSCuPc, confirming the presence of TSCuPc. The weight

percentage of attached TSCuPc is calculated to be about 27%, corresponding to one TSCuPc unit per 220 carbons of GR. Thus, GR-TSCuPc is composed of GR (73%) and TSCuPc (27%) by weight.

ARTICLE

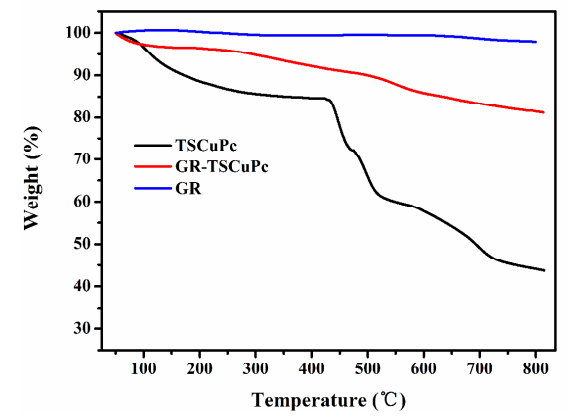


Fig. 5 TGA curves of GR, TSCuPc and GR–TSCuPc recorded at $10\ \Box/min$ under N_2 atmosphere.

To give insight into the structural feature of GR-TSCuPc, the transmission electron microscopy (TEM) measurement was performed. It can be clearly observed that GR-TSCuPc still retains the typical shape of wrinkled GR sheets compared to pristine GR (Fig. 6), which indicates that the non-covalent functionalization with TSCuPc do not significantly change the morphology of GR.

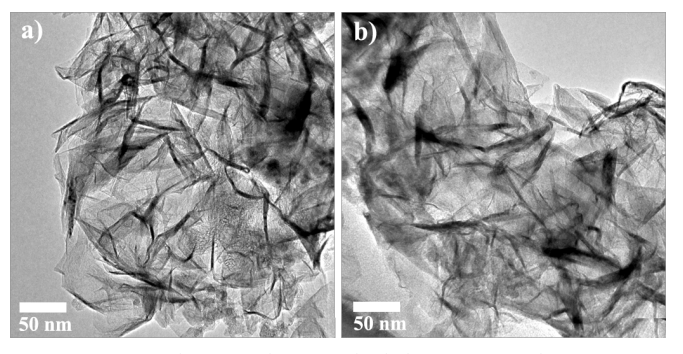


Fig. 6 Representative TEM images of pristine GR (a) and GR-TSCuPc (b).

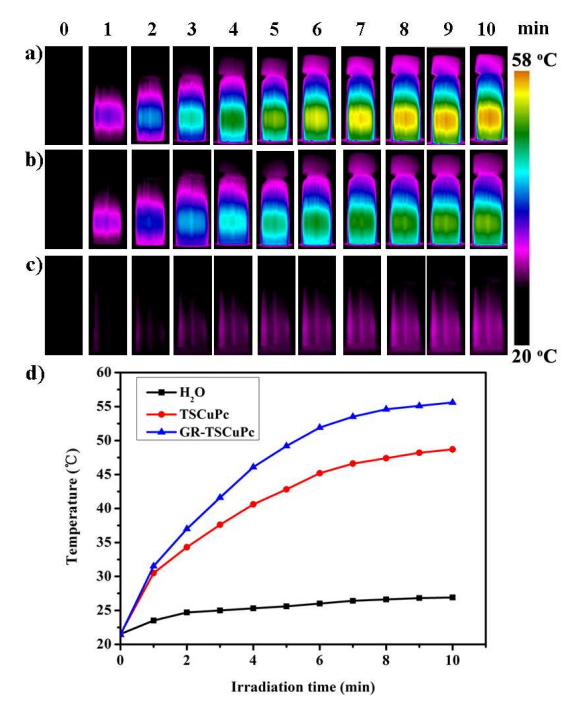


Fig. 7 Photothermal images of GR–TSCuPc solution (a), TSCuPc solution (b) and pure water (c) upon exposure to 650 nm laser (3 W cm $^{-2}$) for different time periods. (d) The corresponding time-dependent photothermal curves of samples. GR–TSCuPc and TSCuPc solution with equivalent TSCuPc concentration of 10 $\mu g\ mL^{-1}$.

Photothermal and photodynamic properties. GR have strong optical absorption in the visible to NIR region and favor photothermal conversion, which make GR ideal for use as photothermal agent.^{22–24} To verify the potential of using GR-TSCuPc in PTT, we detected the temperature elevations of water, free TSCuPc and GR-TSCuPc solutions upon exposure to a laser with a center wavelength of 650 nm and a power density of 3 W cm⁻² by using a thermal imaging camera, respectively. As shown in Fig. 7c and d, no significant temperature change ($\Delta T < 5$ °C) is observed when pure water is exposed to laser light. On the contrary, the temperature of the GR-TSCuPc solution rises with increasing exposure time and can be up by 35 °C, indicating that the GR-TSCuPc can efficiently convert the 650 nm laser energy into thermal energy (Fig. 7a and d). Under the same condition, free TSCuPc also shows temperature change, but which is smaller than that of GR-TSCuPc (Fig. 7b and d). In addition, GR without functionality cannot be dispersed in water, which limits investigation on photothermal effect of GR alone. However, on the combination of the previous reports on photothermal conversion of GR, 8,53,54 such observation can illustrate that both GR and TSCuPc contribute to the ptotothermal effect of GR-TSCuPc upon exposure to 650 nm laser. It is worth mentioning that the combined photothermal effect of GR and TSCuPc makes GR-TSCuPc rapidly heated to over 45 °C within 5 min, capable for cancer cell killing.

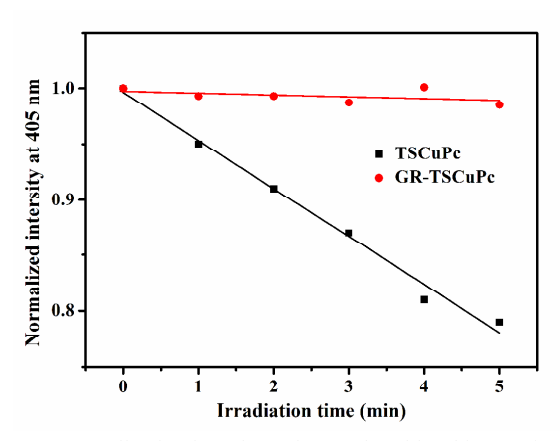


Fig. 8 Normalized time-dependent photobleaching of ADPA fluorescence at 405 nm as singlet oxygen generated by 650 nm laser (3 W cm $^{-2}$) irradiation of TSCuPe and GR $^{-}$ TSCuPe with equivalent TSCuPe concentration of 5 μg mL $^{-1}$ in aqueous solution.

Reactive oxygen species (ROS), such as ¹O₂ or free radicals, are the critical step in PDT, so the ROS generation ability of GR-TSCuPc is a very important index to illustrate its application potential in PDT. We primarily monitored the ability of free TSCuPc and GR-TSCuPc to produce ${}^{1}O_{2}$ by a chemical method using anthracene-9, 10-dipropionic acid disodium salt (ADPA), whose fluorescence intensity would be diminished in the presence of 1O2, owing to production of a non-fluorescent peroxide through reaction of ADPA with ¹O₂. ^{34,55,56} Fig. S3 shows fluorescence spectra of free TSCuPc and GR-TSCuPc as a function of exposure time to a 650 nm laser irradiation. The fluorescence intensity of ADPA displays a continuous decrease within 5 min for free TSCuPc (Fig. 2a and Fig. 8), whereas it shows no fluorescence change for GR-TSCuPc (Fig. S2b and Fig. 8). This means that ${}^{1}O_{2}$ can be generated by the laser irradiation of free TSCuPc but not GR-TSCuPc, similar to previous report of phototherapy system based on carbon nanohorn and phthalocyanine.³⁴

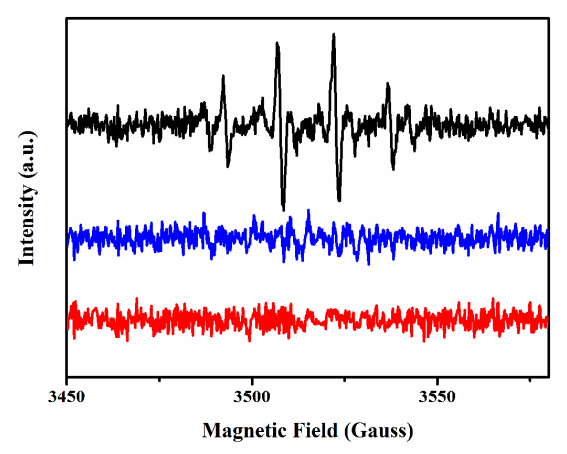
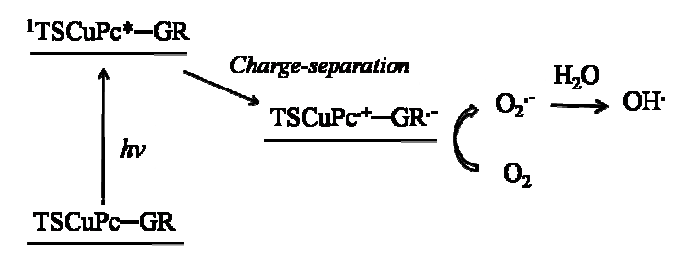


Fig. 9 EPR spectra of DMPO with 650 nm laser irradiation (red line), DMPO and GR-TSCuPc mixture without (blue line) and with 650 nm laser irradiation (black line) in PBS solution.

We further employed the electron paramagnetic resonance (EPR) spin trapping technique to investigate more detailed energy/electron transfer process in GR-TSCuPc, where a

common spin trap reagent (5,5-dimethyl-1-pyrroline-N-oxide, DMPO) was used to detect the $O_2^{\bullet-}$ or OH^{\bullet} . Upon the 650 nm laser irradiation of the GR-TSCuPc, EPR signal of the adduct of DMPO with OH (DMPO-OH adduct) is detected, whereas there is no DMPO-OH adduct signals without laser irradiation (Fig. 9), indicating that laser irradiation of GR-TSCuPc can effectively lead to the formation of OH. Combining the EPR results and previous studies of electron transfer, 40,57 we inferred that when TSCuPc is excited by light, electrons transfer from the excited state of TSCuPc moiety to GR and forms a charge separation state, giving GR*-TSCuPc*+, which further transfers the electrons to surrounding oxygen to generate superoxide radical anion $(O_2^{\bullet-})$ and then $OH^{\bullet, 58,59}$ It should be pointed out that no EPR signals of DMPO-OOH adduct (the adduct of DMPO with O2 •-) is observed in our study, which may be ascribed to the unstable and short-lived properties of DMPO-OOH that decomposes to DMPO-OH. 60,61 With all these results in hand, the possible mechanism of photoinduced process in GR-TSCuPc is schematically illustrated in Scheme 2. The presence of diverse ROS allows us to use GR-TSCuPc for PDT treatment of cancer cells.



Scheme 2. Schematic illustration of the possible photoinduced process for GR–TSCuPc in the presence of O_2 in aqueous solution upon exposure to 650 nm laser.

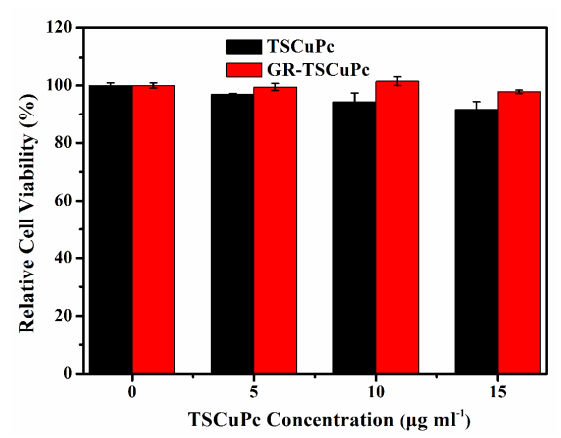


Fig. 10 *In vitro* cell viability of HeLa cells incubated with free TSCuPc and GR–TSCuPc with different TSCuPc concentrations from 0 to 15 μg mL $^{-1}$ for 24 h at 37°C, respectively.

In Vitro therapeutic efficacy of PDT-PTT combined therapy. In order to evaluate the phototherapy effect of GR-TSCuPc, cell viabilities with different treatments were measured. We first examined the dark toxicity of free TSCuPc and GR-TSCuPc at different concentrations of TSCuPc ranging from 0 to 15 mg mL⁻¹ for 24 h by standard MTT assay

in vitro using human cervix cancer cell (HeLa), respectively (Fig. 10). The cell viabilities were higher than 90%, even at the high concentration of 15 mg mL⁻¹. These data show satisfactory results for *in vitro* non-cytotoxicity for all dosages of GR-TSCuPc. Good biocompatibility and low cytotoxicity imply that GR-TSCuPc can serve as a combinatorial PDT/PTT agent of cancer.

ARTICLE

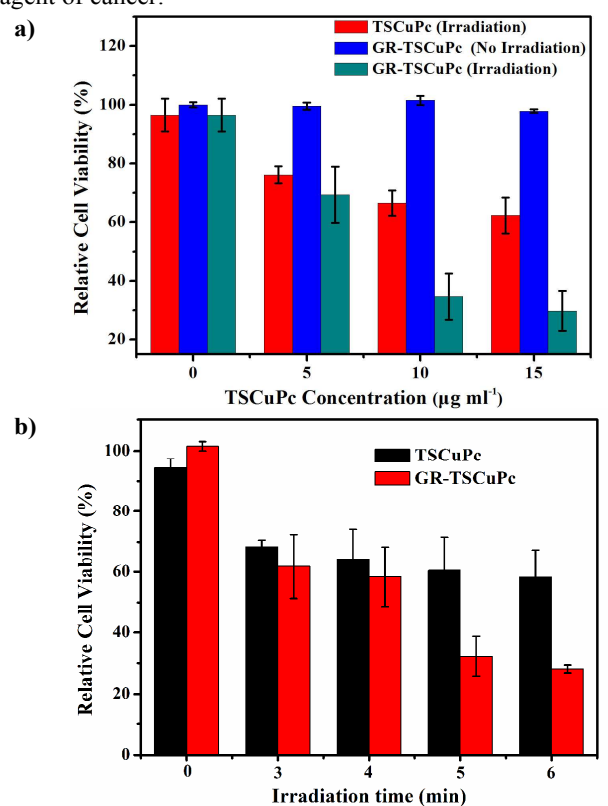


Fig. 11 *In vitro* photodynamic and photothermal cancer cell killing. (a) HeLa cells incubated with free TSCuPc and GR–TSCuPc at different TSCuPc concentrations from 0 to 15 μg mL⁻¹ for 24 h at 37°C, and then irradiated with or without 650 nm laser at a power density of 3 W cm⁻² for 5 min. (b) HeLa cells incubated with free TSCuPc and GR–TSCuPc at equivalent TSCuPc concentration of 10 μg mL⁻¹, and then irradiated for 0 to 6 min.

Furthermore, we determined the in vitro cytotoxicity of PTT and PDT effect of GR-TSCuPc, where HeLa cells were incubated in culture medium containing a series of concentrations of GR-TSCuPc for 24 h, and then irradiated with 650 nm laser for 5 min. As shown in Fig. 11a, without GR-TSCuPc, laser irradiation only shows nearly no damage to HeLa cells, whereas in the presence of GR-TSCuPc, irradiation decreases the cell viability that is remarkably reduced from about 69 to 29% with the TSCuPc concentration from 5 to 15 ug ml⁻¹, showing an obvious phototherapy effect efficacy. Although free TSCuPc can also induce decrease in cell viability (76% ~ 62%), it is evidently much lower than that of GR-TSCuPc. Additionally, the cell viability experiment of GR alone with irradiation is attempted to perform, but restricted owing to insolubility of GR without any functionality. Meanwhile, the cell viability decreases significantly with the increase of irradiation time (Fig. 11b), similar to the

phenomena of cell viability induced by concentration changes that the phototherapy effect of GR–TSCuPc is observably higher than that of free TSCuPc. Therefore, these results indicate that GR–TSCuPc can destroy cancer cells more efficiently compared to free TSCuPc, which can be attributed to dual-modality PTT and PDT arisen from the GR–TSCuPc hybrid. It should be noted that it is lack of direct evidence of phototherapy effect contributed by GR. However, on the basis of the previous studies on PTT of GR, 8,53,54 we can infer that GR indeed contribute to phototherapy effect through photothermal conversion.

Conclusions

In summary, a water-soluble dual-modality therapy system (GR-TSCuPc) for PTT and PDT has been successfully fabricated by a facile one-step method through coating TSCuPc on the surface of GR via non-covalently $\pi-\pi$ interaction. In this PTT/PDT system, both GR and TSCuPc operate as multifunctional agent: GR acts as PS carrier and PTT agent, while TSCuPc simultaneously acts as hydrophilic agent and PDT agent. Further, the results of $in\ vitro\ cell\ viability\ showed$ that the phototherapy effect of GR-TSCuPc is observably higher than that of free TSCuPc, which indicates that dual-modality therapy combined PTT and PDT exhibits better anticancer efficacy. Such results highlight that the combined PTT and PDT endows GR-TSCuPc with the potential promise for cancer theranostics.

Experimental section

Materials

Graphene (GR) sheets (99.95%) used here was prepared by direct current arc-discharge method. Copper (II) phthalocyanine -3,4',4",4"'-tetrasulfonic acid tetrasodium salt (TSCuPc) and 5, 5-dimethyl-1-pyrroline-N-oxide were purchased from Aldrich. All above chemicals were used directly without further purification.

Preparation of GR-TSCuPc

GR (10 mg) was added to TSCuPc aqueous solution (40 mL, 0.5 mg mL $^{-1}$) followed by sonication at 140 W power output for 3 h. Subsequent, the dispersion was centrifuged at 5000 rpm for 30 min to remove larger aggregates, and the ink-like supernatant was collected. After that period, the resultant ink-like solution was filtered through 0.22 μm polytetrafluoroethylene (PTFE) membrane filter, and rinsed with water until the filtrate became colorless, ensuring that no free TSCuPc existed in the precipitate. Finally, the precipitate was re-dissolved in pure water.

The GR-TSCuPc hybrid was fabricated by non-covalently coating TSCuPc on the surface of GR via a facile one-step method, as depicted in Scheme 1. In brief, GR was firstly added to TSCuPc aqueous solution, followed by sonication. Subsequently, the dispersion was centrifuged to remove large aggregates. After that period, the resultant ink-like solution was

filtered, and rinsed with water until the filtrate became colorless, ensuring that no free TSCuPc existed in the precipitate. Finally, the obtained precipitate was re-dissolved in pure water, which was found to be naturally stable with no observable precipitation for months as the GR-TSCuPc hybrid.

Characterizations and instruments.

The morphologies of GR-TSCuPc were studied by transmission electron microscope (TEM, H-600, JEOL, Japan). The UV-vis spectra were recorded on a Cary 100 UV-visible spectrometer. The Raman spectra were measured on Renishaw in Via Raman microscope at 514 nm exciting line, which were taken with 10 seconds of exposure times and 30 percent of power at 20 times of accumulation. X-ray photoelectron spectra (XPS) were obtained with an ESCALAB 250 spectrometer with a monochromatic Al Kα (1486.6 eV) Xray source. Survey and high resolution spectra were recorded at pass energy of the analyzer of 150 and 20 eV, respectively. The binding energies were calibrated to the C 1s binding energy of contamination carbon at 284.8 eV. High resolution spectra were deconvoluted with the Gaussian-Lorentzian mixed function after background subtraction with the Shirley method using the software "XPS peak". Atomic ratios were computed from experimental intensity ratios and normalized by atomic sensitivity factors. TGA (Labsys Evo; Setaram Instruments) was carried out in nitrogen gas at a temperature elevation rate of 10°C/min.

Photothermal activity of graphene

GR–TSCuPc and TSCuPc solutions were diluted to a final concentration of 10 μg mL⁻¹ of TSCuPc equivalent. One milliliter of these solutions were placed in a series of specimen bottles and irradiated by 650 nm laser (3 W cm⁻²), respectively. Light induced temperature change in the solutions were collected every 30 s by using a thermal camera (MAG30, Magnity Electronics, China).

Reactive oxygen species generation

The generation of singlet oxygen by free TSCuPc and GR-TSCuPc was detected using ADPA as the indicator. 150 μ L ADPA solution (100 mM) was added to 2 ml TSCuPc or GR-TSCuPc solution, and irradiated with 650 nm laser (3 W cm⁻²). After irradiation for special time, the fluorescence intensity of ADPA ($\lambda_{\rm exc}$ =376 nm) were measured by time-resolved fluorescence spectroscopy (FL3-P-TCSPS, HORIBA JOBIN JVON, France).

To measure the generation of $O_2^{\bullet-}$ or OH^{\bullet} by GR-TSCuPc, 5,5-dimethyl-1-pyrroline-N-oxide (DMPO) was used as a spin trap reagent. Experimental solution was prepared by mixing 10 μ L GR-TSCuPc (TSCuPc concentration 100 μ g mL⁻¹), 10 μ L DMPO (0.8 M) and 90 10 μ L PBS (pH 7.0). The solution was placed in a quartz cell and irradiated with 650 nm laser (3 W cm⁻²) for 5 min. after that, the solution was inserted into capillary tube and then placed in the EPR cavity, and the spectra were recorded on a Bruker A300 Spectrometer at 298 K. The measurement conditions were as follows. Frequency, 9.8

GHz; microwave power, 19.87 mW; sweep time, 27.65 s; sweep width, 200 G; modulation frequency, 100 kHz.

Phototherapy assay

The in vitro cytotoxicity study was performed using human cervical cancer cell (HeLa cell). Cells were cultured in normal RPMI-1640 culture medium containing 10% fetal bovine serum and 1% penicillin-streptomycin at 37 $\ \square$ under 5% CO_2 . For cytotoxicity assay, HeLa cells were seeded into 96 well cellplates with 10^4 cells per well and incubated at 37 $\ \square$ for 24 h. Then, the cells were treated with free TSCuPc or GR–TSCuPc at a series of concentrations for 24 h. During this time cells were kept in dark without light exposure. After that, 10 μL MTT solution was added to each well and the plate was incubated for another 2 h. The intracellular formazan crystals were extracted into 100 μL DMSO after removing the medium, and then the absorbance at 570 nm was recorded by a microplate reader.

To measure the phototoxicity, cells were seeded as previously. After 24 h incubation, cells were treated with free TSCuPc or GR-TSCuPc at a series of concentrations (0~15 μg mL $^{-1}$ of TSCuPc equivalent) or various irradiation time (10 μg mL $^{-1}$ of TSCuPc equivalent). After 24 h, cells were irradiated with a 650 nm laser (3 W cm $^{-2}$). The cells were incubated for another 24 h and cell viabilities were measured by standard MTT assay.

Acknowledgements

This work was supported by the Natural Science Foundation of China (No. 21161003, 21364002), Guangxi Natural Science Foundation of China (No. 2013GXNSFGA019001, 2012GXNSFDA053007), the Program for New Century Excellent Talents in University of the Ministry of Education (NCET-13-0743), the Program for New Century National Hundred, Thousand and Ten Thousand Talent Project of Guangxi, the State Key Laboratory Cultivation Base for the Chemistry and Molecular Engineering of Medicinal Resources (No. CMEMR2012-A12). We thank Prof. Hui Chao (Sun Yat-Sen University, China) and Haihua Pan (Zhejiang University, China) for kind help with EPR test.

Notes and references

Ministry of Education Key Laboratory for the Chemistry and Molecular Engineering of Medicinal Resources, School of Chemistry and Pharmaceutical Science, Guangxi Normal University, Guilin, 541004, P. R. China Tel: (+86) 773-5846273; E-mail: xcshen@mailbox.gxnu.edu.cn; hliang@gxnu.edu.cn.

Electronic Supplementary Information (ESI) available: [Experimental details and analytical data]. See DOI: 10.1039/b000000x/

- ‡ Contributed equally to this work.
- 1 F. Greco and M. J. Vicent, Adv. Drug. Deliv. Rev., 2009, 61, 1203-1213.
- 2 D. Lane, Nat. Biotechnol., 2006, 24, 163-164.
- 3 N. Kolishetti, S. Dhar, P. M. Valencia, L. Q. Lin, R. Karnik, S. J. Lippard, R. Langer and O. C. Farokhzad, *Proc. Natl. Acad. Sci.*, 2010, 107, 17939–17944.
- 4 C.-M. J. Hu and L. Zhang, Biochem. Pharmacol., 2012, 83, 1104-1111.

- 5 K. Yang, L. Feng, X. Shi and Z. Liu, Chem. Soc. Rev., 2013, 42, 530-547.
- 6 T. J. Dougherty, J. E. Kaufman, A. Goldfarb, K. R. Weishaupt, D. Boyle and A. Mittleman, *Cancer Res.*, 1978, **38**, 2628–2635.
- 7 T. J. Dougherty, C. J. Gomer, B. W. Henderson, G. Jori, D. Kessel, M. Korbelik, J. Moan and Q. Peng, *J. Natl. Cancer Inst.*, 1998, **90**, 889–905.
- 8 E. S. Shibu, M. Hamada, N. Murase and V. Biju, J. Photochem. Photobiol. C: Photochem. Rev., 2013, 15, 53–72.
- L. C. Kennedy, L. R. Bickford, N. A. Lewinski, A. J. Coughlin, Y. Hu, E.
 S. Day, J. L. West and R. A. Drezek, Small, 2011, 7, 169–183.
- 10 A. Sahu, W. I. Choi, J. H. Lee and G. Tae, *Biomaterials*, 2013, 34, 6239–6248.
- 11 J. T. Robinson, S. M. Tabakman, Y. Liang, H. Wang, H. Sanchez Casalongue, D. Vinh and H. Dai, *J. Am. Chem. Soc.*, 2011, **133**, 6825–6831.
- 12 J. F. Lovell, T. W. Liu, J. Chen and G. Zheng, *Chem. Rev.*, 2010, 110, 2839–2857.
- 13 D. E. Dolmans, D. Fukumura and R. K. Jain, *Nat. Rev. Cancer*, 2003, 3, 380–387.
- 14 W. M. Sharman, C. M. Allen and J. E. Van Lier, *Drug Discovery Today*, 1999, 4, 507–517.
- 15 H. Wang, Y. Liang, T. Mirfakhrai, Z. Chen, H. S. Casalongue and H. Dai, Nano Res., 2011, 4, 729–736.
- 16 X. Huang, X. Qi, F. Boey and H. Zhang, Chem. Soc. Rev., 2012, 41, 666–686.
- 17 Q. Cheng, M. Wu, M. Li, L. Jiang and Z. Tang, Angew. Chem., Int. Ed., 2013, 52, 3750-3755.
- 18 Q. Cheng, L. Jiang and Z. Tang, Acc. Chem. Res., 2014, 47, 1256-1266.
- 19 Q. He, S. Wu, Z. Yin and H. Zhang, Chem. Sci., 2012, 3, 1764-1772.
- 20 S. He, B. Song, D. Li, C. Zhu, W. Qi, Y. Wen, L. Wang, S. Song, H. Fang and C. Fan, Adv. Funct. Mater., 2010, 20, 453–459.
- 21 L. A. L. Tang, J. Wang and K. P. Loh, J. Am. Chem. Soc., 2010, 132, 10976–10977.
- 22 Z. M. Markovic, L. M. Harhaji-Trajkovic, B. M. Todorovic-Markovic, D. P. Kepić, K. M. Arsikin, S. P. Jovanović, A. C. Pantovic, M. D. Dramićanin and V. S. Trajkovic, *Biomaterials*, 2011, 32, 1121–1129.
- 23 W. Zhang, Z. Guo, D. Huang, Z. Liu, X. Guo and H. Zhong, *Biomaterials*, 2011, 32, 8555–8561.
- 24 K. Yang, S. Zhang, G. Zhang, X. Sun, S.-T. Lee and Z. Liu, *Nano Lett.*, 2010, 10, 3318–3323.
- 25 B. Tian, C. Wang, S. Zhang, L. Feng and Z. Liu, *ACS Nano*, 2011, **5**, 7000–7009.
- 26 Y. Wang, H. Wang, D. Liu, S. Song, X. Wang and H. Zhang, Biomaterials, 2013, 34, 7715–7724.
- 27 J. P. Mensing, T. Kerdcharoen, C. Sriprachuabwong, A. Wisitsoraat, D. Phokharatkul, T. Lomas and A. Tuantranont, *J. Mater. Chem.*, 2012, 22, 17094–17099.
- 28 X. Zhang, Y. Feng, S. Tang and W. Feng, Carbon, 2010, 48, 211-216.
- 29 X.-F. Zhang and Q. Xi, Carbon, 2011, 49, 3842-3850.
- 30 A. E. O'Connor, W. M. Gallagher and A. T. Byrne, *Photochem. Photobiol.*, 2009, **85**, 1053–1074.
- 31 X. Ma, S. Sreejith and Y. Zhao, ACS Appl. Mater. Interfaces, 2013, 5, 12860–12868.
- 32 S. Dhami and D. Phillips, J. Photochem. Photobiol. A: Chem., 1996, 100, 77–84.
- 33 N. Nombona, K. Maduray, E. Antunes, A. Karsten and T. Nyokong, J. Photochem. Photobiol. B: Biology, 2012, 107, 35–44.

- 34 M. Zhang, T. Murakami, K. Ajima, K. Tsuchida, A. S. Sandanayaka, O. Ito, S. Iijima and M. Yudasaka, Proc. Natl. Acad. Sci., 2008, 105, 14773–14778.
- 35 We did not record the UV-vis spectrum of GR due to its insoluble in water.
- 36 A. Chunder, T. Pal, S. I. Khondaker and L. Zhai, J. Phys. Chem. C, 2010, 114, 15129–15135.
- 37 R. A. Hatton, N. P. Blanchard, V. Stolojan, A. J. Miller and S. R. P. Silva, *Langmuir*, 2007, 23, 6424–6430.
- 38 A. R. Monahan, J. A. Brado and A. F. DeLuca, J. Phys. Chem., 1972, 76, 446–449.
- 39 Y. Wang, H.-Z. Chen, H.-Y. Li and M. Wang, *Mater. Sci. Eng.: B*, 2005, 117, 296–301.
- 40 A. S. Sandanayaka, O. Ito, M. Zhang, K. Ajima, S. Iijima, M. Yudasaka, T. Murakami and K. Tsuchida, *Adv. Mater.*, 2009, **21**, 4366–4371.
- 41 X. Zhang, Y. Feng, S. Tang and W. Feng, Carbon, 2010, 48, 211-216.
- 42 A. Ferrari, J. Meyer, V. Scardaci, C. Casiraghi, M. Lazzeri, F. Mauri, S. Piscanec, D. Jiang, K. Novoselov and S. Roth, *Phys. Rev. Lett.*, 2006, **97**, 187401
- 43 F. Tuinstra and J. L. Koenig, J. Chem. Phys., 2003, 53, 1126-1130.
- 44 D. C. Marcano, D. V. Kosynkin, J. M. Berlin, A. Sinitskii, Z. Sun, A. Slesarev, L. B. Alemany, W. Lu and J. M. Tour, ACS Nano, 2010, 4, 4806–4814.
- 45 N. Inagaki, S. Tasaka and Y. Ikeda, J. Appl. Polym. Sci., 1995, 55, 1451–1464.
- 46 J. Zhang, M. Z. Wu, T. S. Pu, Z. Y. Zhang, R. P. Jin, Z. S. Tong, D. Z. Zhu, D. X. Cao, F. Y. Zhu and J. Q. Cao, Thin solid films, 1997, 307, 14–20.
- 47 D. Zheng, Z. Gao, X. He, F. Zhang and L. Liu, Appl. Surf. Sci., 2003, 211, 24–30
- 48 R. Graupner, J. Abraham, A. Vencelová, T. Seyller, F. Hennrich, M. M. Kappes, A. Hirsch and L. Ley, Phys. Chem. Chem. Phys., 2003, 5, 5472–5476.
- 49 Q. Su, S. Pang, V. Alijani, C. Li, X. Feng and K. Müllen, Adv. Mater., 2009, 21, 3191-3195.
- 50 J.-Q. Zeng, S.-N. Sun, J.-P. Zhong, X.-F. Li, R.-X. Wang, L.-N. Wu, L. Wang and Y.-J. Fan, *Int. J. Hydrogen Energy*, 2014.
- 51 J.-P. Zhong, Y.-J. Fan, H. Wang, R.-X. Wang, L.-L. Fan, X.-C. Shen and Z.-J. Shi, *J. Power Sources*, 2013, **242**, 208–215.
- 52 M. Zhang, C. Shao, Z. Guo, Z. Zhang, J. Mu, T. Cao and Y. Liu, ACS Appl. Mater. Interfaces, 2011, 3, 369-377.
- 53 Z. M. Markovic, L. M. Harhaji-Trajkovic, B. M. Todorovic-Markovic, D. P. Kepić, K. M. Arsikin, S. P. Jovanović, A. C. Pantovic, M. D. Dramićanin and V. S. Trajkovic, *Biomaterials*, 2011, 32, 1121–1129.
- 54 Y. Wang, K. Wang, J. Zhao, X. Liu, J. Bu, X. Yan and R. Huang, J. Am. Chem. Soc. 2013, 135, 4799–4804.
- 55 W. Tang, H. Xu, R. Kopelman and M. A. Philbert, *Photochem. Photobiol.*, 2005, 81, 242–249.
- 56 F. Yan and R. Kopelman, Photochem. Photobiol., 2003, 78, 587–591.
- 57 X.-F. Zhang and Q. Xi, Carbon, 2011, 49, 3842-3850.
- 58 J. M. Matés and F. M. Sánchez-Jiménez, *Int. J. Biochem. Cell Biology*, 2000, **32**, 157–170.
- 59 I. Nakanishi, S. Fukuzumi, T. Konishi, K. Ohkubo, M. Fujitsuka, O. Ito and N. Miyata, J. Phys. Chem. B, 2002, 106, 2372–2380.
- 60 J. Lee, Y. Yamakoshi, J. B. Hughes and J.-H. Kim, Environ. Sci. Technol., 2008, 42, 3459–3464.

61 A. Lipovsky, Z. Tzitrinovich, H. Friedmann, G. Applerot, A. Gedanken and R. Lubart, *J. Phys. Chem. C*, 2009, **113**, 15997–16001.

J. Mater. Chem. B

